Design of the first full size ATLAS ITk Strip sensor for the endcap region

C. Lacasta[c,*], Y. Abo[b], A.A. Affolder[e], V. Fadeyev[e], K. Hara[h], N.P. Hessey[g], S. Kamada[b], R.S. Orr[f], R. Teuscher[f], M. Ullan[a], Y. Unno[d], K. Yamamura[b]

[a] *Centro Nacional de Microelectronica (IMB-CNM, CSIC), Campus UAB-Bellaterra, 08193 Barcelona, Spain*
[b] *Solid State Division, Hamamatsu Photonics K.K., 1126-1, Ichino-cho, Higashi-ku, Hamamatsu-shi, Shizuoka 435-8558, Japan*
[c] *Instituto de Física Corpuscular (IFIC) - CSIC-University of Valencia, Parque Científico, C/Catedrático José Beltrán 2, E-46980 Paterna, Spain*
[d] *IPNS, KEK, 1-1 Oho, Tsukuba, Ibaraki 305-0801, Japan*
[e] *Santa Cruz Institute for Particle Physics (SCIPP), University of California, Santa Cruz, CA 95064, USA*
[f] *Department of Physics, University of Toronto, 60 Saint George St., Toronto M5S 1A7, Ontario, Canada*
[g] *Physical Sciences Division, TRIUMF, 4004 Wesbrook Mall, Vancouver, BC, Canada V6T 2A3*
[h] *Institue of Pure and Applied Sciences, University of Tsukuba, 1-1-1 Tennodai, Tsukuba Ibaraki 305-8571, Japan*

Abstract

The ATLAS collaboration is designing the all–silicon Inner Tracker (ITk) that will operate in the HL-LHC replacing the current design. The silicon microstrip sensors for the barrel and the endcap regions in the ITk are fabricated in 6 inch, p-type, float-zone wafers, where large-area strip sensor designs are laid out together with a number of miniature sensors. The radiation tolerance and specific system issues like the need for slim edge of 450 µm have been tested with square shaped sensors intended for the barrel part of the tracker. This work presents the design of the first full size silicon microstrip sensor for the endcap region with a slim edge of 450 µm. The strip endcaps will consist of several wheels with two layers of silicon strip sensors each. The strips have to lie along the azimuthal direction, apart from a small stereo angle rotation (20 mrad on each side, giving 40 mrad total) for measuring the second coordinate of tracks. This stereo angle is built into the strip layout of the sensor and, in order to avoid orphan strips, the sensor edges are inclined by the stereo angle. On top of this, the top and bottom edges are designed as arcs to have equal length strips. Together with the design of this new *Stereo Annulus* sensor, we will report on the initial measurements of the leakage current as a function of bias voltage, after dicing, and the depletion voltage.

ATL-ITK-PROC-2018-010
20 February 2018

1. Introduction

The ATLAS [1] collaboration will replace the central tracking system for the operation at the High Luminosity LHC (HL-LHC) [2]. The new ATLAS Inner Tracker (ITk) will be operational for more than ten years, during which time ATLAS aims to accumulate a total data set of 4000 fb^{-1}. The ITk will be an all silicon detector formed by an inner pixel system surrounded by the strip sub-detector (Fig. 1.a). The maximum expected fluence in the endcap region of the ATLAS ITk-Strips in the HL-LHC is anticipated to be about 2×10^{15} 1 MeV n_{eq}/cm^2 [3]. These fluences include a safety factor of two in the estimation.

The current design of the ITk-Strips detector has 4 cylinders in the barrel and two 1.5 m long endcap cylinders at each side [4]. Each of the cylinders houses 6 wheels as shown in Fig. 1.b. All the wheels in the endcap will cover from an inner radius of 385 mm to 970 mm and will be made of 32 identical petals. The petals are carbon fibre sandwiches that combine the mechanical support with all the required services for a completely autonomous multi-module system. These double sided objects have 9 sensors on each side, as depicted in Fig. 1.c, organised in six rings. There is a different sensor shape per ring. The upper three rings in the petal have two equal sensors while the innermost rings contain only one sensor. Rings are named from lowest to highest radius as R0, R1, ... , R5.

The sensors on the petals should provide a measurement of the azimuthal angle, ϕ, and the radius, R. The strips in the sensors have to lie along the azimuthal direction apart from a small stereo angle,to provide the measurement of R

*Corresponding author. e-mail: carlos.lacasta@ific.uv.es

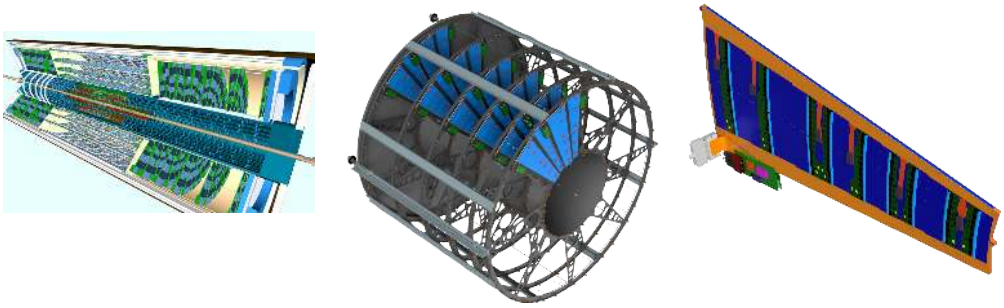

(a) (b) (c)

Figure 1: (a) ATLAS ITk layout showing the pixel and strip systems. (b) The ITk strips endcap showing the six disks and how the petals are arranged in the disks. Note, however, that only 4 petals per disk are shown in the picture. (c) This is a petal where the 9 modules on the front side are shown. Six rings can be appreciated in the picture. Each ring has a different sensor shape. The three outermost rings will contain two identical sensors while the innermost three only one.

by correlating the particle hits on both sides of the petal. The 40 mrad stereo angle between strips on opposite sides of a petal is achieved by rotating the strips 20 mrad within the sensors.

The strip lengths are chosen to balance the strip occupancy with the shortest strips closest to the beam region. This results in sensors having either 2 or 4 strip rows. The strip pitch was constrained to be as close as possible to 75.5 µm at the bond pad region to allow direct wire bonding between the read-out ASIC and the sensor.

Finally, in order to reduce the size of the gaps produced by the sensor separation and the guard region (500 µm and 2×450 µm respectively), the whole sensor assembly in each side of the petal is rotated by 3.5 mrad around the beam axis.

2. The Endcap ITk-Strips sensor design

The silicon strip sensors for the ATLAS ITk-Strips detector will have n^+–type readout implants on a p–type, float–zone silicon substrate (n^+–in–p FZ). The strips are AC coupled and biased with polysilicon resistors. Inter-strip isolation will be achieved by p–stop implants. The target thickness is around 310 µm. This type of sensor has no radiation induced type inversion and electrons drift towards the readout implants allowing to operate in partial depletion and resulting in a much higher signal after irradiation [5].

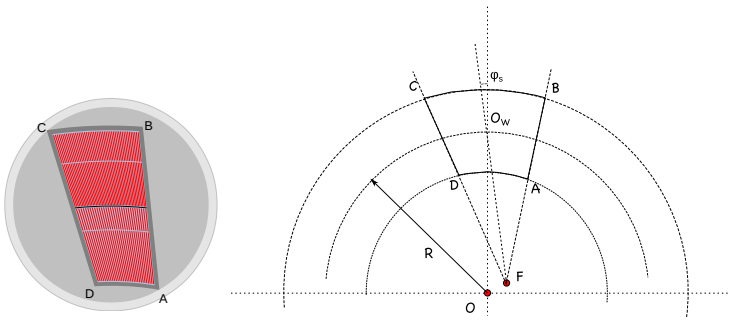

Figure 2: Sensor geometry. The sensors are laid out in a 6-inch wafer so that the area employed is maximal. In the figure, A, B, C and D are the corners of the sensor, φ_S is the built–in stereo angle, O is the center of the wheel and F is where to strips point to.

The petal sensors require radial strips (i.e. pointing to the beam-axis) to give a measurement of the $r\phi$ coordinate. As a result, these sensors have a wedge shape with curved edges. We call the shape *Stereo Annulus* (see Fig. 2): the inner and outer edges are concentric arcs of circles, centred at the centre of the wheel, to cover part of an annulus. The

two sides are straight, but do not point to the centre of the wheel. Instead they are rotated away from the wheel centre by the stereo angle.

The dimensions of the sensors have been chosen to use as few silicon wafers as possible with 32 petals per disk and fully covering the radial range required by the layout. Fig. 2 shows how the geometry of a sensor in a given ring is determined: since a φ_S=20 mrad stereo angle is built within the sensor, strips do not point to the interaction point but rather to a slightly displaced point F. To avoid truncated or orphan strips [12, 13] the sensor lateral edges are parallel to the last strips. Sensors have several rows of strips. Each row has a multiple of 128 strips to match the readout chip number of input channels. Rows come in pairs with equal number of strips in each row of the pair. Bonding pads lie close to the boundary between the two rows of a pair. The strip-ends away from the bonding pads are connected to bias-rails. All strips within a strip row start and end on circular arcs centred in the beam axis (O) as do the sensor upper and lower edges. The angle, or angular pitch, between any two neighbouring strips in a row is constant.

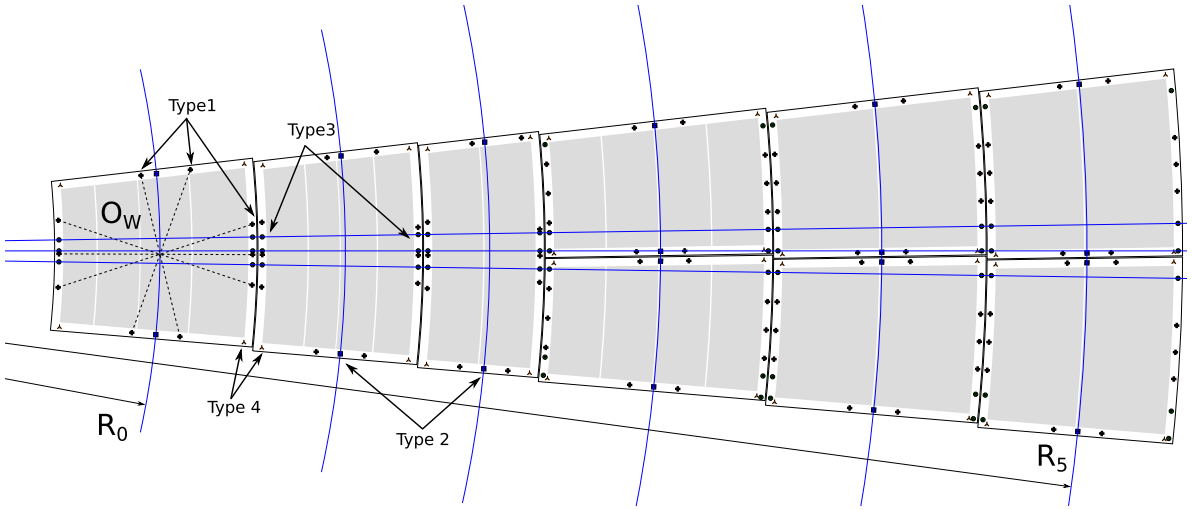

Figure 3: Location of fiducial markers. There are four sets of fiducial markers which are sketched in the picture with different colours: some of the markers (type 1/red) will determine the centre of the sensor, others (type 2/blue) will determine the radius of the sensor in the global system and the last set (type3/green) will help locating the sensors in angle. There is a last set of markers (type 4/brown) at the corners of the sensitive area of the sensor.

2.1. Fiducial markers in the sensor

The sensor will have four sets of fiducial markers each serving different purposes. All the markers are at a distance δ=95 µm from the outermost structure of the sensor. Their location and purpose are sketched in Fig. 3:

- Type 1 fiducial markers to determine the sensor center (O_W). These are located along the arcs defined by the outer and inner radius and on the straight sides of the sensor. They are shown in Fig. 3 as red, thick plus (✚) marks. The markers define lines whose crossing point is the sensor centre (see R0 in Fig. 3).

- Type 2 fiducial markers. They are located along the straight sides of the sensor and are used to define, together with the sensor center, the sensor radius and origin or interacion point (O). They are shown as squares (⊞) in Fig. 3 where a blue arc centered at the origin with the corresponding sensor radius is drawn to guide the view.

- Type 3 fiducial markers to help position the sensor on the petal face. These markers are determined by three lines crossing at the interaction point. The middle line defines the X axis and the other two are at a constant angle ($0.15 \times \pi/32$) from that one. They serve to define the angle of the final sensor position and, together with R and O, determine the position of the sensor in the petal. They are shown as green ⊗ symbols in Fig. 3 together with the straight lines in blue.

- Type 4 fiducial markers are located at the corners of the sensitive region. They are shown as triangles (△) in Fig. 3.

Row	Length (mm)	I–pitch (μm)	O–pitch (μm)	pitch (μrad)
0	18.981	74.314	77.983	193.2745
1	23.981	77.983	82.617	193.2745
2	28.981	73.454	78.434	171.8368
3	31.981	78.434	83.929	171.8368

Table 2: Parameters of the four rows in the R0 sensor. The first two have the same angular pitch as do the last two rows. I–pitch corresponds to the pitch at the inner end of the strip while O–pitch at the outer end of the strip.

3. The R0 sensors

We have been improving the design of the silicon microstrip sensors for the ATLAS ITk-Strips system with barrel (squared) sensors [6]. This is the first time that large area endcap sensors have been fabricated for the ITk-Strips. In order to test the technology we decided to implement the R0 sensor ATLAS12EC–R0. This sensor shape was chosen among the 6 choices cause it has four strip rows and it is complex enough to be used as a validator of the concept. One of the things to validate was the circular dicing. The arcs at the upper and bottom edges of the sensors were approximated by a polygon made of 16 flats. Flats are carefully chosen so that petal HV isolation between neighbouring sensors is ensured without unnecessarily large gaps.

The motivation for the geometry of the sensor is explained in section 2. On top of those geometrical considerations, the sensors were fabricated with an edge space of 450 μm which has been measured to be the minimum for holding a bias voltage of 1 kV initially and as radiation damage accumulated [6]. Also inherited from the ATLAS12 results [7] is the *full-gate* PTP (punch-through-protection) which is the protection of the AC-coupling capacitor, formed with the strip implant and the strip metal, when the voltages at both sides have large excursions as in the case of an accidental beam splash. The specifications of the ATLAS12EC–R0 sensors are summarised in Table 1.

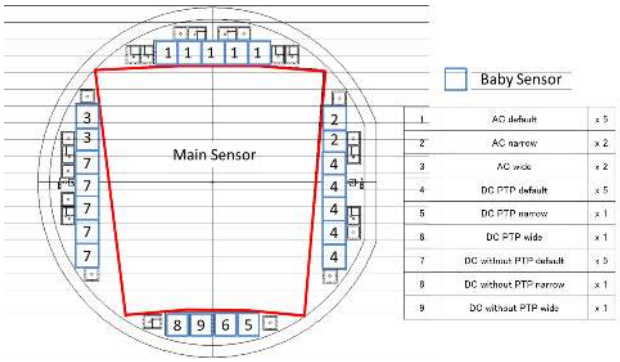

Figure 4: ATLAS12EC–R0 wafer layout in a 6 inch wafer. The miniature sensors are numbered according to the type as explained in the table by the picture.

Sensor Specifications	**ATLAS12EC**
Wafer size	150 mm
Thickness	(310 ± 25) μm
Cristal Orientation	<100>
Wafer Type	p–type FZ
Resistivity	> 3 kΩ cm
Strip segments	4
Strip implant	n–type
Strip implant Width	16 μm
Strip bias resistance (R_b, polysilicon)	(1.5 ± 0.5) MΩ
Strip readout coupling	AC
Strip readout metal	Pure Aluminium
Strip readout metal width	20 μm
Strip AC coupling capacitance	> 20 pF cm^{-1}
Strip isolation	> 10×R_b at 300 V
Strip isolation method	Narrow–common p–stop
Punch Through Protection (PTP)	Gated
Gap between strip segments	56 μm (rail region) 70 μm (no rail region)
Microdischarge onset voltage	> 600 V
Maximum operation voltage	700 V
Leakage current	< 2 μA cm^{-2}

Table 1: Specicifations of the ATLAS12EC–R0 large area silicon microstrip sensors.

Table 2 shows the dimensions of the strips in the four rows. It also shows the angular pitch and the strip pitch. As already said, strip rows come in pairs and bonding pads are in the region between the two rows in a pair. This is where O–pitch of the inner row should more or less match I–pitch of the outer and the value should be close to the nominal 75.5 μm which is optimal to match the readout ASIC.

Fig. 4 shows the wafer layout. Apart from the large area sensor there are 23 miniature sensors. These are $10 \times 10\,\mathrm{mm}^2$, rectangular devices which have a design similar to the main sensors. They have been designed to have different strip coupling (DC and AC), strip pitch (narrow: 70 μm, default: 75.5 μm, wide: 84 μm) and, in the case of the DC coupling they are also produced with and without PTP structure.

Fig. 5 shows the main dimensions of the ATLAS12EC–R0 large area sensor. It only shows the two innermost strip rows. One can appreciate the size and location of the AC bonding pads as well as the DC pads used for testing single

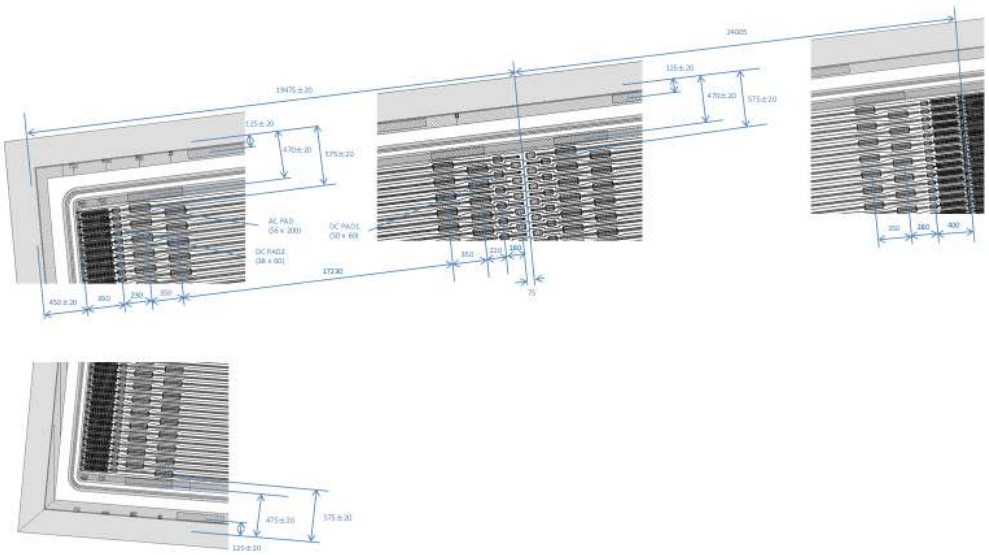

Figure 5: Dimensions of the ATLAS12EC–R0 large area sensor. The picture shows the innermost two rows.

strips. One can also appreciate the dimension of the gap between the two strip rows, where there is no bias rail, and the connection to the bias rail at the left and right of the image.

4. Initial performance of the ATLAS12EC–R0 sensors

A total of 155 of these sensors have been fabricated so far by Hammatsu Photonics K.K. [8] using p–type FZ wafers with a physical thickness of 320 µm. A measurement campaign to validate the quality of the process was made on a sample of all the sensors. A thorough program to study the properties of this sensors has been started and first results are shown in other talks of this conference, in particular for the technology parameters of the sensor [9], charge collection efficiency [10] or the performance in a module for the ATLAS ITk-Strips module [11].

This paper shows the data measured by the vendor. Fig. 6.a shows the leakage current as a function of the bias voltage. Most of the sensors demonstrated no breakdown in leakage current up to 1000 V with very low leakage current of the order of 1 nA cm^{-2} at room temperature.

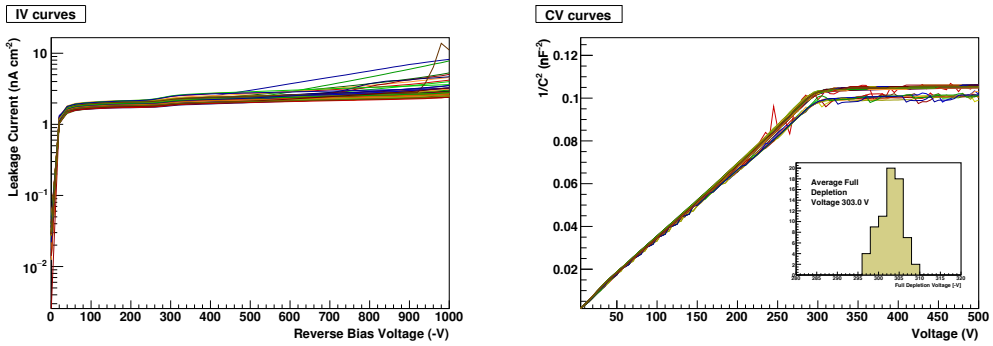

(a) (b)

Figure 6: IV and CV curves measured in the ATLAS12EC–R0 sensors. The IV curves are normalised to 20 °C and to the bias ring area. Also shown in the right plot is the distribution of the measured full depletion voltage V_{FD}.

Fig. 6.b shows the value of the inverse of the bulk capacitance squared as a function of the reverse bias voltage. All the curves are very similar. From these curves the full depletion voltage, V_{FD}, can be measured since it corresponds to the crossing point of the plateau and the slope at lower voltages. Fig. 6.b also shows the distribution of V_{FD} that, on average, is around 303 V. An average of C=3.09 nF is obtained from the CV–plot for the bulk capacitance. From this value, for a sensor of 90 cm^2, the active thickness is w = 305.8 μm and the wafer resistivity is ρ = 3.27 kΩ cm.

5. Summary

We have been developing sensors suitable for the ATLAS ITk-Strips detector to be operated in the HL-LHC environment. We have designed and fabricated large area sensors for the ITK-Strips endcap region where 6 different sensor shapes need to be designed and used. This work shows the design and first results of the very first of those sensors, the one closest to the interaction point: the R0 sensor.

The concept of the sensors for the ITK-Strips endcaps have been proven to be feasible. We have fabricated 155 of those sensors with circular dicing and built–in stereo angle. The first measurements made to characterize the technology parameters of the fabrication process show that those sensors perform very well. Most of the sensors exhibit no breakdown in leakage current up to 1000 V. The leakage currents measured are of the order of 1 nA cm^{-2} measured at room temperature. Measurements of the capacitance as a function of the bias voltage show that the full depletion voltage is around 303 V, the average wafer active thickness is 305.8 μm and the wafer resistivity is 3.27 kΩ cm.

6. Acknowledgements

The research was supported and financed in part by Canada Foundation for Innovation, the National Science and Engineering Research Council (NSERC) of Canada under the Research and Technology Instrumentation (RTI) grant SAPEQ-2016-00015; the Spanish Ministry of Economy and Competitiveness through the Particle Physics National Program, ref. FPA2015-65652-C4-4-R (MINECO/FEDER, UE), and co-financed with FEDER funds; and USA Department of Energy, Grant DE-SC0010107.

7. References

[1] ATLAS Collaboration, The ATLAS Experiment at the CERN Large Hadron Collider, JINST 3 (2008) S08003.
[2] G. Apollinari et al. High-Luminosity Large Hadron Collider (HL-LHC): Preliminary Design Report. doi:10.5170/CERN-2015-005, 2015.
[3] P. S. Miyagawa and I. Dawson, Radiation background studies for the Phase II inner tracker upgrade, Tech. Rep. ATL-UPGRADE-PUB-2013-012, CERN, 2013. https://cds.cern.ch/record/1516824.
[4] ATLAS Collaboration, Technical Design Report for the ATLAS Inner Tracker Strip Detector, CERN-LHCC-2017-005. April 2017.
[5] K. Hara et al., Testing of bulk radiation damage of n-in-p silicon sensors for very high radiation environments, Nucl. Instr. Meth. Phys. Res. A636 (2011) S83S89.
[6] Y. Unno et al., Development of n+-in-p large-area silicon microstrip sensors for very high radiation environments ATLAS12 design and initial results, Nucl. Instr. Meth. Phys. Res. A765 (2014) 80 90.
[7] S. Mitsui, et al., Nuclear Instruments and Methods in Physics Research Section A 699 (2013) 36.
[8] Hamamatsu Photonics K.K., http://www.hamamatsu.com.
[9] R. Hunter et al., First bulk and surface results for the ATLAS ITk Strip stereo annulus sensors, HSTD11 & SOIPIX. December 2017.
[10] V. Cindro et al., Measurement of charge collection in irradiated miniature sensors for the upgrade of ATLAS Phase-II Strip tracker, HSTD11 & SOIPIX. December 2017.
[11] C. García Argos et al., Assembly and Electrical Tests of the First Full-size Forward Module for the ATLAS ITk Strip Detector, HSTD11 & SOIPIX. December 2017.
[12] V. Benítez et al. "Sensors for the End-cap prototype of the Inner Tracker in the ATLAS Detector Upgrade", NIMA 833 (2016) 226-232.
[13] R. Mori et al. "Evaluation of the performance of irradiated silicon strip sensors for the forward detector of the ATLAS Inner Tracker Upgrade", NIMA 831 (2016) 2017-212.